Wavelet-domain de-noising of OCT images of human brain malignant glioma

I.N. Dolganova[a], P.V. Aleksandrova[a], S.-I.T. Beshplav[b], N.V. Chernomyrdin[a,d,h], E.N. Dubyanskaya[c], S.A. Goryaynov[b], V.N. Kurlov[c], I.V. Reshetov[d], A.A. Potapov[b], V.V. Tuchin[e,f,g], and K.I. Zaytsev[a,d,h]

[a]Bauman Moscow State Technical University, Moscow 105005, Russia
[b]Burdenko Neurosurgery Institute, Moscow 125047, Russia
[c]Institute of Solid State Physics of RAS, Chernogolovka 142432, Russia
[d]Sechenov First Moscow State Medical University, Moscow 119991, Russia
[e]Saratov State University, Saratov 410012, Russia
[f]Institute of Precision Mechanics and Control of RAS, Saratov 410028, Russia
[g]Tomsk State University, Tomsk 634050, Russia
[h]Prokhorov General Physics Institute of RAS, Moscow 119991, Russia

ABSTRACT

We have proposed a wavelet-domain de-noising technique for imaging of human brain malignant glioma by optical coherence tomography (OCT). It implies OCT image decomposition using the direct fast wavelet transform, thresholding of the obtained wavelet spectrum and further inverse fast wavelet transform for image reconstruction. By selecting both wavelet basis and thresholding procedure, we have found an optimal wavelet filter, which application improves differentiation of the considered brain tissue classes – i.e. malignant glioma and normal/intact tissue. Namely, it allows reducing the scattering noise in the OCT images and retaining signal decrement for each tissue class. Therefore, the observed results reveals the wavelet-domain de-noising as a prospective tool for improved characterization of biological tissue using the OCT.

Keywords: optical coherence tomography, brain tumor, malignant glioma, scattering noise, wavelet analysis

1. INTRODUCTION

Optical coherence tomography (OCT) was introduced by Huang *et al*[1] in 1991. Many research have shown, that OCT becomes an effective noninvasive imaging technique for many fields of biomedical applications, providing necessary and important information about internal tissue structure and its scattering properties.[2,3] Numerous research in ophthalmology,[4–8] vascular and blood imaging,[9,10] dermatology,[11,12] prostate pathology,[13] reproductive methods,[14] detecting malignant tissues and cancer cells,[15–20] neuroscience[19–23] were done using OCT techniques. OCT is based on the principles of low-coherence interferometry either in time-domain or frequency domain.[24–29] Using visual and infrared radiation sources, OCT can be combined with endoscopic approaches for exploring hidden tissues. Besides, such techniques as Doppler and polarization-sensitive OCT are also widely applied for biomedical imaging.[30]

Recent *in vitro* and *in vivo* studies in neurosurgery demonstrate that OCT could become an important imaging technique.[15,23] Comparing it with the existed and developing methods, such as intraoperative magnetic resonance imaging,[31–33] THz reflectometry,[34,35] Raman spectroscopy,[36–38] and fluorescence imaging,[39–41] OCT combines fast and noninvasive analysis of tissue structure, its scattering and polarization properties. One of the most promising application of OCT in neurosurgery is imaging of brain tumors, such as malignant glioma.[15,23,35,42] Glioma appears in almost 30% cases of human brain tumor diagnosis and in 80% of malignant cases.[42] Complete resection of glioma tissue is a key-reason for the successful treatment, thus, the necessity of accurate differentiation

Further author information:
I.N.D.: E-mail: in.dolganova@gmail.com; K.I.Z.: E-mail: kirzay@gmail.com

Saratov Fall Meeting 2017: Laser Physics and Photonics XVIII; and Computational Biophysics and Analysis of Biomedical Data IV, edited by Vladimir L. Derbov, Dmitry E. Postnov, Proc. of SPIE Vol. 10717, 107171X · © 2018 SPIE · CCC code: 1605-7422/18/$18 · doi: 10.1117/12.2314727

of tumor area from surrounding intact brain tissue is of high importance. Meanwhile, most of tissues, including brain, are highly scattering media for OCT, accordingly, scattering noise leads to significant image distortion.[43,44] Therefore, in order to improve differentiation between the considered tissues, an appropriate noise suppression technique should be applied.

Several post-processing approaches are available in OCT-imaging, including averaging and filtering procedures,[45–53] among which wavelet de-noising yields significant results.[47–49,53] The effectiveness of wavelet filtration procedure is mainly explained by the similar physical features of wavelet kernels and optical wave packets: zero means value, finite energy corresponding to square norm one, and high locality in both time- and frequency-domains .

In the present paper, we suggest using wavelet-domain de-nosing procedure for the filtration of malignant brain glioma and intact tissue images obtained by OCT. We apply selection between different wavelet basis and thresholding methods in order to determine optimal wavelet filter parameters. We demonstrate that applying this wavelet filter it is possible to reduce scattering noise and retain OCT-signal decrement, and yield better differentiation of the considered tissue classes.

2. WAVELET-DOMAIN DE-NOISING PROCEDURE

Wavelet-domain de-noising procedure includes the following stages: image decomposition by the direct wavelet transformation, thresholding of the obtained wavelet spectrum, and image reconstruction by the inverse wavelet transformation. For the OCT-signal – light intensity $I(x, z)$ scattered from the object, these procedures can be applied separately to different cross-sections $I_{\mathrm{x}}(z) = I(x = x', z)$. Here, z is the sample depth and x is the lateral coordinate. Using the mother wavelet $\psi(z)$ we obtain the wavelet-decomposition kernels $\psi(a, b, z)$ for scale and translation parameters a and b

$$\psi(a, b, z) = |a|^{-1/2} \psi\left(\frac{z-b}{a}\right). \tag{1}$$

Then direct wavelet transform

$$C(a, b) = \mathcal{W}[I(z)] = \int_{-\infty}^{+\infty} I_{\mathrm{x}}(z)\, \psi(a, b, z)\, dz, \tag{2}$$

is followed by the thresholding of the wavelet-spectrum with T value

$$C_{\mathrm{T}}(a, b) = \begin{cases} C(a, b), & \text{if} \quad C(a, b) \geq T, \\ 0, & \text{if} \quad C(a, b) < T. \end{cases} \tag{3}$$

The dual functions $\widetilde{\psi}(a, b, z)$ of $\psi(a, b, z)$ are used for the inverse wavelet-transform

$$I'_{\mathrm{x}}(z) = \mathcal{W}^{-1}[C_{\mathrm{T}}(a, b)] = C_{\psi}^{-1} \iint_{-\infty}^{+\infty} \frac{C_{\mathrm{T}}(a, b)}{a^2} \widetilde{\psi}(a, b, z) da db, \tag{4}$$

where the admissible constant

$$C_{\psi} = \int_{-\infty}^{+\infty} \frac{\Psi(\omega)\widetilde{\Psi}(\omega)}{|\omega|} d\omega < \infty \tag{5}$$

restricts the diversity of functions suitable for definition of mother wavelet $\psi(z)$. Here, functions $\Psi(\omega)$ and $\widetilde{\Psi}(\omega)$ in (5) correspond to Fourier spectra of $\psi(z)$ and $\widetilde{\psi}(z)$, respectively.

In order to process the data of OCT imaging, in this paper, we apply methods of fast direct and inverse wavelet transforms[54] (FDWT and FIWT) and consider "soft" and "hard" thresholding modalities,[55,56] and different number of decomposition levels L.

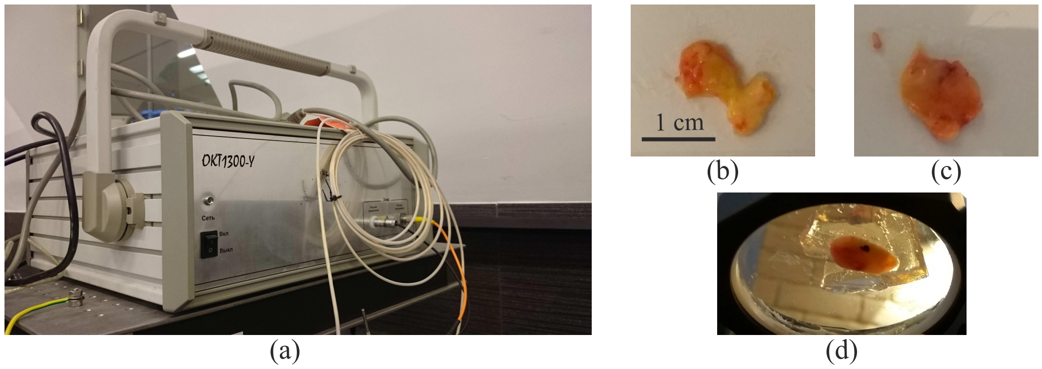

Figure 1. *In vitro* OCT-imaging of brain tissue samples: (a) a photo of OCT time-domain system OCT1300Y; (b), (c) examples of studied samples of malignant brain glioma and intact tissue; (d) tissue sample placed on glass and covered with gelatin layer for preventing its hydration/dehydration during imaging.

3. DE-NOISING OF THE BRAIN TISSUE OCT-IMAGES

In order to obtain sample-images, we use OCT1300Y-system (Institute of Applied Physics RAS, Nizny Novgorod, Russia), which is shown in Fig. 1(a). It operates in near-infrared range and employs radiation source with a central wavelength of 1.3 μm and an average power up to 6 mW. It allows for performing A- and B-scans of the sample and produces 256x400 pixels images with 4 sec acquisition time. The theoretical estimation of the approximate OCT system resolution is 50 μm in lateral and 30 μm in depth directions. The optical depth of sample probing is near 1...2 mm.

The samples of human brain intact tissue and malignant glioma (Fig. 1(b) and (c)) were explored no later than 4 hours after neurosurgery. To fix each tissue, prevent its hydration/dehydration, and sustain its structure and composition during both transportation and OCT-imaging, we placed the tissue samples on a reference optically-transparent substrate and cover them with gelatin films.[57] All the examined tissues samples were excited according to the initial medical diagnosis. After OCT-imaging, all samples were fixed in formalin and sent to histological examination, which result confirmed initial diagnosis and verified the results of OCT experimental study.

Initial OCT-images of glioma and intact tissue are demonstrated in Fig. 2 (a) and (b). The normalized OCT-signal averaged for 350 A-scans $I(z)$, where z is optical scanning depth, is shown in Fig. 2 (c). Since two tissue types are characterized by different signal decrements, we find a width parameter L at $1/e$ level and

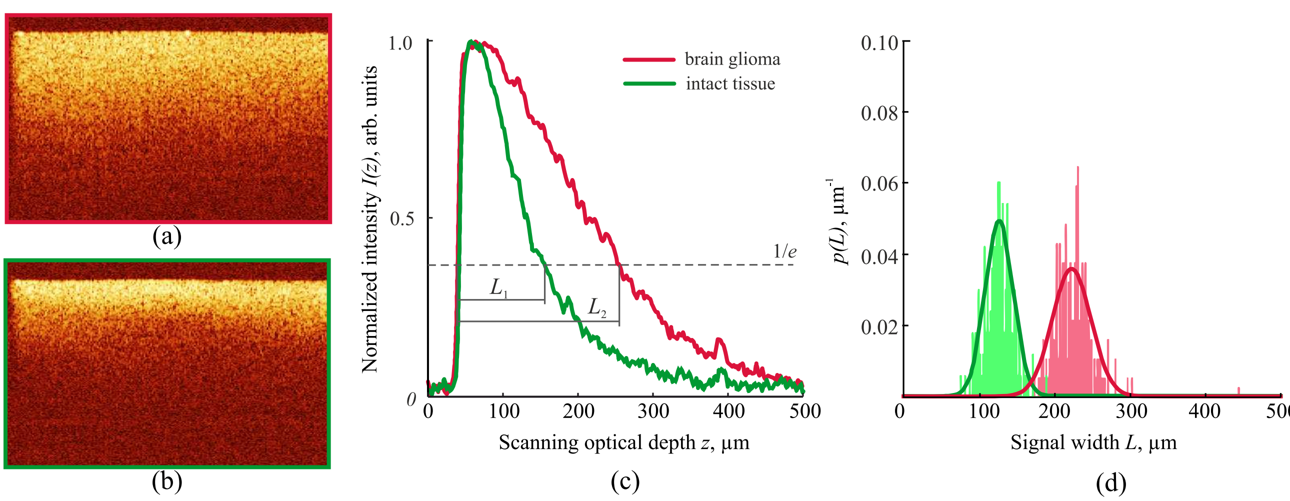

Figure 2. OCT-images of human brain tissue: (a) malignant glioma, (b) intact region; (c) normalized averaged intensity $I(z)$, (d) probability density function of signal width L with corresponding normal distribution assumption.

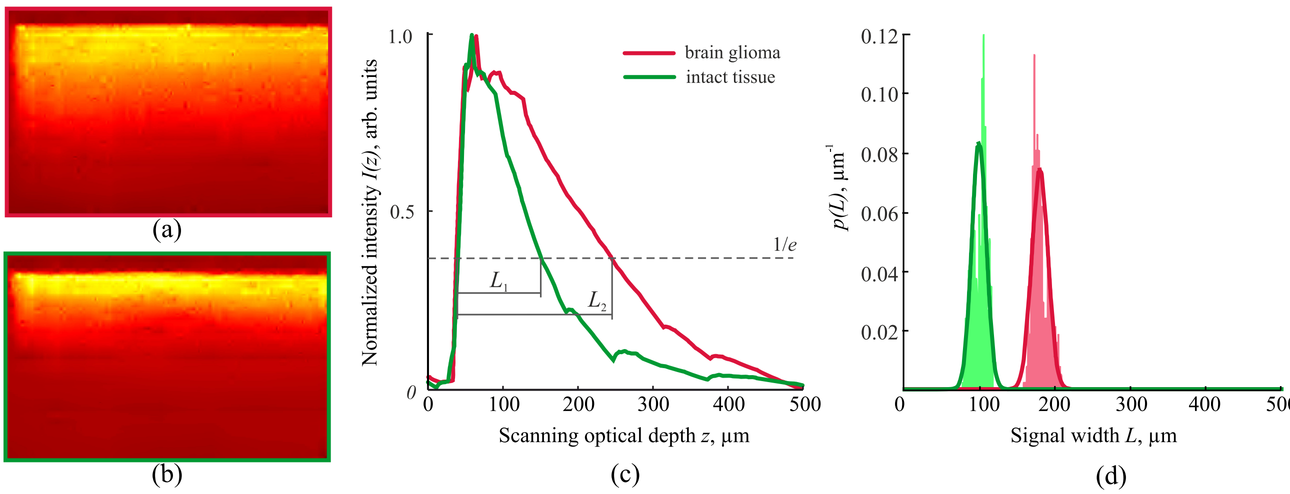

Figure 3. Results of wavelet de-noising procedure with Daubechie-kernel filter for OCT-images of human brain tissue: (a) malignant glioma, (b) intact region; (c) normalized averaged intensity $I(z)$, (d) probability density function of signal width L with corresponding normal distribution assumption.

the probability density function $p(L)$, assuming its normal (Gaussian) character. These estimations for the considered samples are shown on panel (d). Using the determined mean value M and standard deviation σ of the obtained signal statistics, we calculate a separability parameter of two classes $k = (\mathrm{M}_1 - \mathrm{M}_2)(1/\sigma_1 + 1/\sigma_2)$. For the demonstrated images the value of k is equal to 9.2.

We apply wavelet-domain de-noising procedure described in Sec. 2 using several wavelet basis (Daubechies, Coiflets, Symlets, Biorthogonal, and Reverse Biorthogonal) and thresholding techniques, and select optimal ones (Daubechie-type *db2* with "soft" thresholding and decomposition level equal to 8), which yield higher value of $k = 16.9$. The results of this filter application is demonstrated in Fig. 3. The filtered images are characterized with more smooth signal intensity and significant noise suppression. Meanwhile, de-noising procedure does not result in changes of signal width comparing to the initial images. Therefore, analysis of signal width probability density function due to less dispersion leads to better differentiation between brain tissue classes.

Designed and tested de-noising technique should be useful at application of tissue optical clearing to enhance probing depth and image contrast[28,29,58,59] We may expect synergetic effect from optical clearing used together with signal filtering.

In case of other brain tissue types, for example, meningioma, with its highly heterogeneous internal structure, other parameters and wavelet-domain de-noising filters should be proposed, which could be based on special morphological and scattering features of each type of tissue. Nevertheless, combining OCT-imaging technique with an appropriate wavelet filtration procedure, it is possible to increase the efficiency of brain tumor visualization.

4. CONCLUSION

We have demonstrated the application of wavelet-domain de-noising procedure for OCT-imaging of human brain malignant glioma and its differentiation from intact brain tissue. For OCT-images of these tissue samples, we applied de-noising procedure varying filter parameters: wavelet basis, thresholding method, and decomposition level, and optimized them for better differentiation of the considered tissue classes. The obtained results of using *db2*-wavelet with "soft" thresholding and decomposition level equal to 8 yields almost two-times increase of the classification efficiency.

ACKNOWLEDGMENTS

Data processing done by I.N.D and N.V.C was supported by the Russian Science Foundation, Project No. 14-19-01083. Experimental studies done by V.V.T. were supported by the Ministry of Education and Science of the Russian Federation, Grant No. 17.1223.2017/AP. Samples were prepared by S.-I.T.B, S.A.G, A.A.P.

REFERENCES

[1] Huang, D., Swanson, E., Lin, C., Schuman, J., Stinson, W., Chang, W., Hee, M., Flotte, T., Gregory, K., Puliafito, C., and et al., "Optical coherence tomography," *Science* **254**(5035), 1178–1181 (1991).

[2] Tuchin, V. V., "Tissue optics and photonics: Biological tissue structures [review]," *Journal of Biomedical Photonics and Engineering* **1-2**(1-3) (2015-2016).

[3] Tuchin, V. V., "Polarized light interaction with tissues," *Journal of Biomedical Optics* **21**(7), 071114–21–37 (2016).

[4] Puliafito, C. A., Hee, M. R., Lin, C. P., Reichel, E., Schuman, J. S., Duker, J. S., Izatt, J. A., Swanson, E. A., and Fujimoto, J. G., "Imaging of macular diseases with optical coherence tomography," *Ophtalmology* **102**(2), 217–229 (1995).

[5] Fujimoto, J. G., "Optical coherence tomography for ultrahigh resolution in vivo imaging," *Nature Biotechnology* **21**(11), 1361 – 1367 (2003).

[6] Bagayev, S. N., Gelikonov, V. M., Gelikonov, G. V., Kargapoltsev, E. S., Kuranov, R. V., Razhev, A. M., Turchin, I. V., and Zhupikov, A. A., "Optical coherence tomography for in situ monitoring of laser corneal ablation," *Journal of Biomedical Optics* **7**(4), 633–642 (2002).

[7] Sonka, M. and Abràmoff, M. D., "Quantitative analysis of retinal OCT," *Medical Image Analysis* **33**, 165 – 169 (2016).

[8] Cua, M., Lee, S., Miao, D., Ju, M. J., Mackenzie, P. J., Jian, Y., and Sarunic, M. V., "Retinal optical coherence tomography at 1 μm with dynamic focus control and axial motion tracking," *Journal of Biomedical Optics* **21**(2), 026007 (2016).

[9] Yabushita, H., Bouma, B. E., Houser, S. L., Aretz, H. T., Jang, I.-K., Schlendorf, K. H., Kauffman, C. R., Shishkov, M., Kang, D.-H., Halpern, E. F., and Tearney, G. J., "Characterization of human atherosclerosis by optical coherence tomography," *Circulation* **106**(13), 1640–1645 (2002).

[10] Winetraub, Y., SoRelle, E. D., Liba, O., and de la Zerda, A., "Quantitative contrast-enhanced optical coherence tomography," *Applied Physics Letters* **108**(2) (2016).

[11] Welzel, J., "Optical coherence tomography in dermatology: a review," *Skin Research and Technology* **7**(1), 1–9 (2001).

[12] Shlivko, I. L., Kirillin, M. Y., Donchenko, E. V., Ellinsky, D. O., Garanina, O. E., Neznakhina, M. S., Agrba, P. D., and Kamensky, V. A., "Identification of layers in optical coherence tomography of skin: comparative analysis of experimental and Monte Carlo simulated images," *Skin Research and Technology* **21**(4), 419–425 (2015).

[13] Muller, B. G., de Bruin, D. M., van den Bos, W., Brandt, M. J., Velu, J. F., Bus, M. T. J., Faber, D. J., Savci, D., Zondervan, P. J., de Reijke, T. M., Pes, P. L., de la Rosette, J., and van Leeuwen, T. G., "Prostate cancer diagnosis: the feasibility of needle-based optical coherence tomography," *Journal of Medical Imaging* **2**(3), 037501 (2015).

[14] Zarnescu, L., Leung, M. C., Abeyta, M., Sudkamp, H., Baer, T., Behr, B., and Ellerbee, A. K., "Label-free characterization of vitrification-induced morphology changes in single-cell embryos with full-field optical coherence tomography," *Journal of Biomedical Optics* **20**(9), 096004 (2015).

[15] Kut, C., Chaichana, K. L., Xi, J., Raza, S. M., Ye, X., McVeigh, E. R., Rodriguez, F. J., Quiñones-Hinojosa, A., and Li, X., "Detection of human brain cancer infiltration ex vivo and in vivo using quantitative optical coherence tomography," *Science Translational Medicine* **7**(292), 292ra100 (2015).

[16] Zhu, Y., Gao, W., Zhou, Y., Guo, Y., Guo, F., and He, Y., "Rapid and high-resolution imaging of human liver specimens by full-field optical coherence tomography," *Journal of Biomedical Optics* **20**(11), 116010 (2015).

[17] Tsai, M. T., Lee, J. D., Lee, Y. J., Lee, C. K., Jin, H. L., Chang, F. Y., Hu, K. Y., Wu, C. P., Chiang, C. P., and Yang, C. C., "Differentiation of oral precancerous stages with optical coherence tomography based on the evaluation of optical scattering properties of oral mucosae," *Laser Physics* **23**(4), 045602 (2013).

[18] Avanaki, M. R. N., Hojjatoleslami, A., Sira, M., Schofield, J. B., Jones, C., and Podoleanu, A. G., "Investigation of basal cell carcinoma using dynamic focus optical coherence tomography," *Applied Optics* **52**(10), 2116–2124 (2013).

[19] Assayag, O., Grieve, K., Devaux, B., Harms, F., Pallud, J., Chretien, F., Boccara, C., and Varlet, P., "Imaging of non-tumorous and tumorous human brain tissues with full-field optical coherence tomography," *NeuroImage: Clinical* **2**(Supplement C), 549 – 557 (2013).

[20] Lenz, M., Krug, R., Welp, H., Schmieder, K., and Hofmann, M. R., "Ex vivo brain tumor analysis using spectroscopic optical coherence tomography," *Proc. SPIE* **9697**, 9697 – 4 (2016).

[21] Lichtenegger, A., Harper, D. J., Augustin, M., Eugui, P., Muck, M., Gesperger, J., Hitzenberger, C. K., Woehrer, A., and Baumann, B., "Spectroscopic imaging with spectral domain visible light optical coherence microscopy in Alzheimer's disease brain samples," *Biomedical Optics Express* **8**(9), 4007–4025 (2017).

[22] Baran, U. and Wang, R. K., "Review of optical coherence tomography based angiography in neuroscience," *Neurophotonics* **3**(1), 010902 (2016).

[23] Yashin, K. S., Kiseleva, E. B., Gubarkova, E. V., Matveev, L. A., Karabut, M. M., Elagin, V. V., Sirotkina, M. A., Medyanik, I. A., Kravets, L. Y., and Gladkova, N. D., "Multimodal optical coherence tomography for in vivo imaging of brain tissue structure and microvascular network at glioblastoma," *Proc. SPIE* **10050**, 10050 – 7 (2017).

[24] Tuchin, V. V., [*Handbook of Coherent-Domain Optical Methods*], Springer, New York, USA (2013).

[25] Wojtkowski, M., "High-speed optical coherence tomography: basics and applications," *Applied Optics* **49**(16), D30–D61 (2010).

[26] Tearney, G. J., Brezinski, M. E., Bouma, B. E., Boppart, S. A., Pitris, C., Southern, J. F., and Fujimoto, J. G., "In vivo endoscopic optical biopsy with optical coherence tomography," *Science* **276**(5321), 2037–2039 (1997).

[27] Drexler, W., Morgner, U., Kärtner, F. X., Pitris, C., Boppart, S. A., Li, X. D., Ippen, E. P., and Fujimoto, J. G., "In vivo ultrahigh-resolution optical coherence tomography," *Optics Letters* **24**(17), 1221–1223 (1999).

[28] Tuchin, V. V., [*Tissue Optics: Light Scattering Methods and Instruments for Medical Diagnostics, 3rd ed.*], vol. PM 254, SPIE Press, Bellingham, WA (2015).

[29] Khlebtsov, N. G., Maksimova, I. L., Meglinski, I. V., Wang, L., and Tuchin, V. V., [*Handbook of Optical Biomedical Diagnostics. Light-Tissue Interaction, 2nd ed.*], vol. PM 262, SPIE Press, Bellingham, WA (2016).

[30] Fercher, A. F., Drexler, W., Hitzenberger, C. K., and Lasser, T., "Optical coherence tomography – principles and applications," *Reports on Progress in Physics* **66**(2), 239 (2003).

[31] Trantakis, C., Tittgemeyer, M., Schneider, J.-P., Lindner, D., Winkler, D., Strau, G., and Meixensberger, J., "Investigation of time-dependency of intracranial brain shift and its relation to the extent of tumor removal using intra-operative MRI," *Neurological Research* **25**(1), 9–12 (2003).

[32] Senft, C., Bink, A., Franz, K., Vatter, H., Gasser, T., and Seifert, V., "Intraoperative MRI guidance and extent of resection in glioma surgery: a randomised, controlled trial," *The Lancet Oncology* **12**(11), 997 – 1003 (2011).

[33] Schatlo, B., Fandino, J., Smoll, N. R., Wetzel, O., Remonda, L., Marbacher, S., Perrig, W., Landolt, H., and Fathi, A.-R., "Outcomes after combined use of intraoperative MRI and 5-aminolevulinic acid in high-grade glioma surgery," *Neuro-Oncology* **17**(12), 1560–1567 (2015).

[34] Yamaguchi, S., Fukushi, Y., Kubota, O., Itsuji, T., Ouchi, T., and Yamamoto, S., "Brain tumor imaging of rat fresh tissue using terahertz spectroscopy," *Scientific Reports* **6**, 30124 (2016).

[35] Ji, Y. B., Oh, S. J., Kang, S.-G., Heo, J., Kim, S.-H., Choi, Y., Song, S., Son, H. Y., Kim, S. H., Lee, J. H., Haam, S. J., Huh, Y. M., Chang, J. H., Joo, C., and Suh, J.-S., "Terahertz reflectometry imaging for low and high grade gliomas," *Scientific Reports* **6**, 36040 (2016).

[36] Kircher, M. F., de la Zerda, A., Jokerst, J. V., Zavaleta, C. L., Kempen, P. J., Mittra, E., Pitter, K., Huang, R., Campos, C., Habte, F., Sinclair, R., Brennan, C. W., Mellinghoff, I. K., Holland, E. C., and Gambhir, S. S., "A brain tumor molecular imaging strategy using a new triple-modality MRI-Photoacoustic-Raman nanoparticle," *Nature Medicine* **18**, 829834 (2012).

[37] Orringer, D. A., Pandian, B., Niknafs, Y. S., Hollon, T. C., Boyle, J., Lewis, S., Garrard, M., Hervey-Jumper, S. L., Garton, H. J. L., Maher, C. O., Heth, J. A., Sagher, O., Wilkinson, D. A., Snuderl, M., Venneti, S., Ramkissoon, S. H., McFadden, K. A., Fisher-Hubbard, A., Lieberman, A. P., Johnson, T. D., Xie, X. S., Trautman, J. K., Freudiger, C. W., and Camelo-Piragua, S., "Rapid intraoperative histology of unprocessed surgical specimens via fibre-laser-based stimulated Raman scattering microscopy," *Nature Biomedical Engineering* **1**, 0027 (2017).

[38] Jermyn, M., Mok, K., Mercier, J., Desroches, J., Pichette, J., Saint-Arnaud, K., Bernstein, L., Guiot, M.-C., Petrecca, K., and Leblond, F., "Intraoperative brain cancer detection with raman spectroscopy in humans," *Science Translational Medicine* **7**(274), 274ra19 (2015).

[39] Pustogarov, N., Panteleev, D., Goryaynov, S. A., Ryabova, A. V., Rybalkina, E. Y., Revishchin, A., Potapov, A. A., and Pavlova, G., "Hiding in the shadows: CPOX expression and 5-ALA induced fluorescence in human glioma cells," *Molecular Neurobiology* **54**(7), 5699–5708 (2017).

[40] Potapov, A. A., Goryaynov, S. A., Okhlopkov, V. A., Shishkina, L. V., Loschenov, V. B., Savelieva, T. A., Golbin, D. A., Chumakova, A. P., Goldberg, M. F., Varyukhina, M. D., and Spallone, A., "Laser biospectroscopy and 5-ALA fluorescence navigation as a helpful tool in the meningioma resection," *Neurosurgical Review* **39**(3), 437–447 (2016).

[41] Roessler, K., Becherer, A., Donat, M., Cejna, M., and Zachenhofer, I., "Intraoperative tissue fluorescence using 5-aminolevolinic acid (5-ALA) is more sensitive than contrast MRI or amino acid positron emission tomography (18F-FET PET) in glioblastoma surgery," *Neurological Research* **34**(3), 314–317 (2012).

[42] Ostrom, Q. T., Gittleman, H., Xu, J., Kromer, C., Wolinsky, Y., Kruchko, C., and Barnholtz-Sloan, J. S., "Cbtrus statistical report: Primary brain and other central nervous system tumors diagnosed in the united states in 2009-2013," *Neuro-Oncology* **18**, v1–v75 (2016).

[43] Semyachkina-Glushkovskaya, O., Abdurashitov, A., Pavlov, A., Shirokov, A., Navolokin, N., Pavlova, O., Gekalyuk, A., Ulanova, M., Shushunova, N., Bodrova, A., Saranceva, E., Khorovodov, A., Agranovich, I., Fedorova, V., Sagatova, M., Shareef, A. E., Zhang, C., Zhu, D., and Tuchin, V., "Laser speckle imaging and wavelet analysis of cerebral blood flow associated with the opening of the blood–brain barrier by sound," *Chinese Optics Letters* **15**(9), 090002 (2017).

[44] Almasian, M., van Leeuwen, T. G., and Faber, D. J., "OCT amplitude and speckle statistics of discrete random media," *Scientific Reports* **7**, 14873 (2017).

[45] Ozcan, A., Bilenca, A., Desjardins, A. E., Bouma, B. E., and Tearney, G. J., "Speckle reduction in optical coherence tomography images using digital filtering," *Journal of Optical Society of America A* **24**, 1901–1910 (Jul 2007).

[46] Aum, J., Kim, J., and Jeong, J., "Effective speckle noise suppression in optical coherence tomography images using nonlocal means denoising filter with double gaussian anisotropic kernels," *Applied Optics* **54**(13), D43–D50 (2015).

[47] Adler, D. C., Ko, T. H., and Fujimoto, J. G., "Speckle reduction in optical coherence tomography images by use of a spatially adaptive wavelet filter," *Optics Letters* **29**(24), 2878–2880 (2004).

[48] Buranachai, C., Thavarungkul, P., Kanatharanaa, P., and Meglinski, I. V., "Application of wavelet analysis in optical coherence tomography for obscured pattern recognition," *Laser Physics Letters* **6**(12), 892 (2009).

[49] Mayer, M. A., Borsdorf, A., Wagner, M., Hornegger, J., Mardin, C. Y., and Tornow, R. P., "Wavelet denoising of multiframe optical coherence tomography data," *Biomedical Optics Express* **3**(3), 572–589 (2012).

[50] Alonso-Caneiro, D., Read, S. A., and Collins, M. J., "Speckle reduction in optical coherence tomography imaging by affine-motion image registration," *Journal of Biomedical Optics* **16**(11), 116027–116027–5 (2011).

[51] Rogowska, J. and Brezinski, M. E., "Image processing techniques for noise removal, enhancement and segmentation of cartilage OCT images," *Physics in Medicine and Biology* **47**(4), 641 (2002).

[52] Li, M., Idoughi, R., Choudhury, B., and Heidrich, W., "Statistical model for OCT image denoising," *Biomedical Optics Express* **8**(9), 3903–3917 (2017).

[53] Pavlov, A. N., Nazimov, A. I., Pavlova, O. N., Lychagov, V. V., Tuchin, V. V., Bibikova, O. A., Sindeev, S. S., and Semyachkina-Glushkovskaya, O. V., "Wavelet-based analysis of cerebrovascular dynamics in newborn rats with intracranial hemorrhages," *Journal of Innovative Optical Health Sciences* **07**(01), 1350055 (2014).

[54] Mallat, S. G., "A theory for multiresolution signal decomposition: the wavelet representation," *IEEE Transactions on Pattern Analysis and Machine Intelligence* **11**(7), 674–693 (1989).

[55] Donoho, D. L. and Johnstone, J. M., "Ideal spatial adaptation by wavelet shrinkage," *Biometrika* **81**(3), 425–455 (1993).

[56] Donoho, D. L., "De-noising by soft-thresholding," *IEEE Transactions on Information Theory* **41**(3), 613–627 (1995).

[57] Fan, S., Ung, B., Parrott, E. P. J., and Pickwell-MacPherson, E., "Gelatin embedding: a novel way to preserve biological samples for terahertz imaging and spectroscopy," *Physics in Medicine and Biology* **60**(7), 2703 (2015).

[58] Wang, H., Magnain, C., Wang, R., Dubb, J., Varjabedian, A., Tirrell, L. S., Stevens, A., Augustinack, J. C., Konukoglu, E., Aganj, I., Frosch, M. P., Schmahmann, J. D., Fischl, B., and Boas, D. A., "as-PSOCT: Volumetric microscopic imaging of human brain architecture and connectivity," *NeuroImage* (2017).

[59] Larin, K. V., Ghosn, M. G., Bashkatov, A. N., Genina, E. A., Trunina, N. A., and Tuchin, V. V., "Optical clearing for OCT image enhancement and in-depth monitoring of molecular diffusion," *IEEE Journal of Selected Topics in Quantum Electronics* **18**(3), 1244–1259 (2012).